inorganics

MDPI

Article

Unsymmetrical Bis(thiosemicarbazone) Ligands and Their Nickel(II) Complexes: Synthesis, Characterization and Photocatalytic Activity

Rodrigo Burón, David G. Calatayud, M. A. Mendiola and Elena López-Torres *

Departamento de Química Inorgánica, Universidad Autónoma de Madrid, Cantoblanco, 28049 Madrid, Spain; rodrigo.buron@estudiante.uam.es (R.B.); david.gcalatayud@uam.es (D.G.C.); antonia.mendiola@uam.es (M.A.M.)
* Correspondence: elena.lopez@uam.es

Abstract: The widespread use of organic dyes in industrial processes has led to a considerable release of these compounds into water systems, making the removal of organic contaminants from freshwater a pressing challenge. Photocatalysis, particularly through coordination compounds, presents a promising solution to this problem. In this study, we report the synthesis and characterization of three novel dissymmetric bis(thiosemicarbazone) ligands and their corresponding nickel(II) complexes, which have been extensively analyzed using various techniques. We evaluated the photocatalytic degradation of methyl orange by these nickel complexes, with results demonstrating that they exhibit superior efficiency compared to previously reported nickel-based complexes. Theoretical calculations reveal a correlation between the HOMO–LUMO energy gap and the energies of the involved orbitals. Additionally, with the growing demand for sustainable fuels that do not contribute to greenhouse gas emissions, molecular hydrogen stands out as a promising candidate. Given the potential of bis(thiosemicarbazone) complexes for electrocatalytic hydrogen evolution, we performed preliminary experiments to assess the ability of these nickel complexes to function as photocatalysts for water splitting. The results show that the three nickel complexes successfully generate hydrogen under the tested conditions, although further optimization is necessary to improve hydrogen production efficiency.

Keywords: thiosemicarbazones; nickel; electrocatalysis; HER

Academic Editors: Wolfgang Linert, Debbie Crans and David Morales-Morales

Received: 28 November 2024
Revised: 22 January 2025
Accepted: 24 January 2025
Published: 29 January 2025

Citation: Burón, R.; Calatayud, D.G.; Mendiola, M.A.; López-Torres, E. Unsymmetrical Bis(thiosemicarbazone) Ligands and Their Nickel(II) Complexes: Synthesis, Characterization and Photocatalytic Activity. *Inorganics* **2025**, *13*, 40. https://doi.org/10.3390/inorganics13020040

1. Introduction

The world is grappling with significant water and air pollution issues. According to the World Health Organization (WHO), only 5.8 billion people had access to safely managed drinking-water services in 2020 [1]. Organic dyes, extensively used in various industries, are among the most prevalent contaminants, linked to respiratory toxicity and cancer [2,3]. Traditional methods for dye removal, such as precipitation, coagulation, adsorption, filtration, membrane separation, and biodegradation, are often unsatisfactory due to high costs and the need for harmless processing [4–7]. To address this, photocatalytic approaches are being developed to degrade and mineralize toxic organic dyes into less harmful compounds like H_2O, CO_2 and NO_3^- [8–10], and transition metal-based coordination compounds have shown promise in enhancing photocatalytic efficiency [11–13].

Despite thiosemicarbazones being strong chelating ligands and that they have been extensively investigated due to their notable biological activities, such as antimicrobial [14], antitumor [15,16] and hypoxic selectivity [17], the potential of TSC complexes to act as catalysts in diverse reactions has been barely investigated, and they are almost restricted to

different organic reactions such as alkylations or coupling reactions [18,19]. Recently, they have also emerged as promising catalysts in hydrogen evolution reactions (HERs) [20,21], which are critical for sustainable energy production and the development of hydrogen as a clean fuel. Nevertheless, the potential use of TSC complexes in degrading organic dyes has hardly been studied.

Research has shown that thiosemicarbazones can be modified to improve their catalytic performance, such as by altering substituents on the terminal nitrogen or optimizing the metal coordination environment [22]. These modifications can enhance their ability to lower the activation energy required for hydrogen evolution, thereby increasing the efficiency of the reaction. Their versatility allows for the exploration of various metal–thiosemicarbazone complexes, leading to a wide range of catalytic behaviors and efficiencies. Therefore, thiosemicarbazone complexes represent a novel and effective approach for catalyzing hydrogen evolution reactions. Their unique structural features and ability to form stable metal complexes make them valuable in the ongoing pursuit of efficient, sustainable hydrogen production technologies.

Bis(thiosemicarbazones) offer enhanced stability due to their higher denticity and formation of more chelate rings. Dissymmetric bis(thiosemicarbazones) are particularly intriguing, as they can incorporate diverse functional groups, contributing varied electronic and structural properties. However, synthesizing these ligands is challenging, requiring two successive condensation reactions, which increases the risk of undesired by-products. Our research group has focused on designing and synthesizing unsymmetrical ligands with thiocarbazone moieties, developing methods to obtain these ligands with high purity and yield [23,24].

In this paper, we present the synthesis and characterization of three ligands and their nickel(II) complexes. We investigate their potential as photocatalysts for methyl orange degradation and use theoretical calculations to explain our findings. Additionally, we conduct preliminary tests on the photoactivity of the nickel complexes for water splitting reactions, inspired by recent reports on their electrocatalytic activity in HER [25–27].

2. Results and Discussion

For the synthesis of the three ligands, three steps were carried out (Scheme 1). First, the corresponding commercial isothiocyanate reacted with hydrazine monohydrate to obtain the thiosemicarbazide, which was then reacted with an excess of commercial 2,3-butanedione to obtain the monoketones HANfTs, HAClPhTs and HAOMePhTs. Finally, the monoketones were reacted with commercial thiocarbohydrazide to yield L^1H_2, L^2H_2 and L^3H_2.

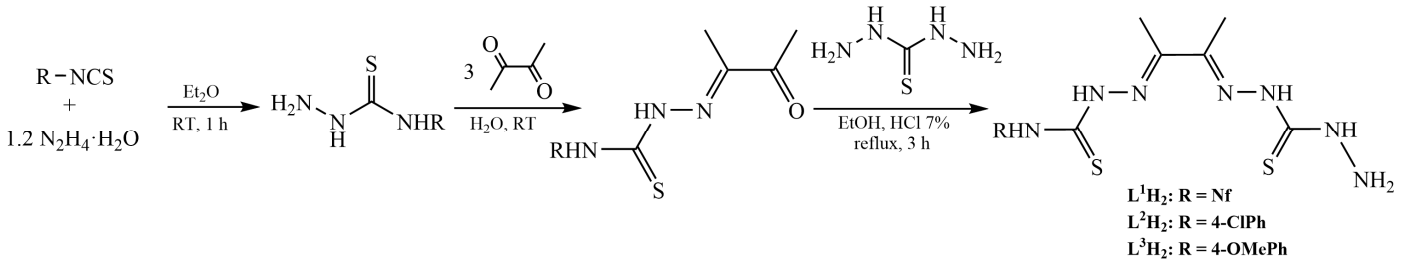

Scheme 1. Synthesis of the ligands.

One of the most important steps of synthesis is the obtaining of the monoketones since secondary reactions can occur such as the double condensation of carbonyls, forming symmetrical bis(thiosemicarbazones), or the formation of unwanted species such as 1,2,4-triazines-3-thiones by cyclization of the monoketones. To avoid these problems, the

synthesis is carried out with a 1:3 excess of 2,3-butanedione (diacetyl). This excess is not a problem because water is used as the solvent for the reaction, and monoketones, being totally insoluble in water, precipitate as soon as they form preventing cyclization, while diacetyl is highly miscible and can be easily removed by successive washes with water. Even with this excess of diacetyl, the formation of the triazine is not always completely avoided, and sometimes, a scarce amount can be isolated from the mother liquor. This happened in the synthesis of HAClPhTS in which crystals of the triazine were obtained. In addition, and due to the presence of two equally reactive NH_2 groups in thiocarbohydrazide, double condensation can occur with two monoketone molecules, which can be avoided using 7% hydrochloric acid instead of concentrated.

Reaction of the ligands with nickel(II) nitrate hexahydrate affords three nickel complexes with high purity and yield (Scheme 2). Even in the absence of a base, the ligand deprotonates spontaneously, which is due to the great tendency of nickel(II) to form square-planar complexes with this type of ligand that can easily accommodate the four donor atoms in a plane. This is the behavior observed for almost all the nickel(II) complexes we have synthesized with our tetradentate ligands, for which it is very difficult to avoid ligand deprotonation. The elemental analysis shows the absence of nitrate anions and, therefore, the doubly deprotonation of the dissymmetric ligands. In the mass spectra, the base peaks correspond to $[M+H]^+$, confirming the formation of the complexes. The peaks of higher mass are due to strong hydrogen bonds, and are usually observed in monomeric square-planar nickel(II) bis(thiosemicarbazonato) complexes [28].

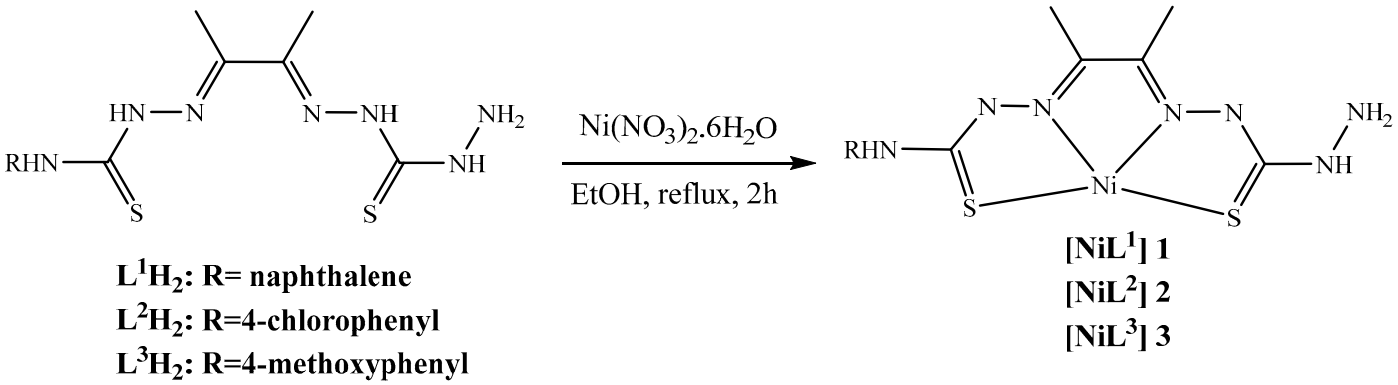

Scheme 2. Synthesis of the nickel(II) complexes.

2.1. Infrared Spectroscopy

In the IR spectra of the three ligands, the strong band around 1685 cm^{-1} present in the monoketones disappears after the formation of the second imine bond with thiocarbohydrazide. In addition, there are more signals in the υ(NH) region, suggesting condensation of only one of the NH_2 groups of thiocarbohydrazide.

Thiosemicarbazones may have tautomeric thione–thiol equilibrium. In all three ligands, the thiol form is discarded since the characteristic band corresponding to υ(S-H) around 2600 cm^{-1} is not observed.

In the IR of the complexes a decrease in the number of υ(NH) bands can be observed, together with the absence of bands attributable to nitrate ions, mainly a strong one around 1385 cm^{-1}, which agrees with the double deprotonation of the ligands. Coordination of a ligand to a metal center should involve a shift of the bands corresponding to the functional groups involved in thiosemicarbazones, the iminic and thione moieties. Nevertheless, this is not always observed and the shift most of the time is difficult to rationalize since these ligands present a great deal of electronic delocalization, highly increased after de-

protonation. In the IR spectra of complexes **1–3**, the bands corresponding to ν(C=N) and ν(C=S) are shifted due to their coordination to the nickel. The only exception is the ν(C=N) in complex **1**, which is almost in the same position, but the N_2S_2 coordination mode is proposed.

2.2. UV-Vis Spectroscopy

The electronic spectra of the three ligands and their complex were recorded in DMF solutions. Two different concentrations were used, 10^{-5} M for the ligands and to analyze the CT bands of the complexes, and 10^{-3} M for the *d-d* transitions of the complexes. The spectra of the three ligands show a band around 340 nm corresponding to a $\pi \rightarrow \pi^*$ charge transfer band and another one around 430 nm, corresponding to a $n \rightarrow \pi^*$ transition. In the spectra of the complexes, these two charge transfer bands can also be observed, but with a hypsochromic effect for the first one and a bathochromic effect for the second. This, together with the appearance of a *d-d* transition around 684 nm, confirms nickel coordination, and is in agreement with the bands observed for other square-planar nickel(II) complexes with bis(thiosemicarbazone) ligands reported in the literature [26,29].

2.3. NMR Spectroscopy

The ^{1}H NMR spectra of the ligands show the signals corresponding to their structures, with the expected integrals and multiplicities. In solution, thione–thiol tautomerism in the ligands results in duplicate signals. This is not observed, so the tautomeric equilibrium is also ruled out, and the ligands remain in the thione form. The presence of a broad singlet around 5 ppm can be noted for two protons corresponding to the unreacted NH_2 group of thiocarbohydrazone. In the spectra of **1–3**, the disappearance of the signals of the hydrazinic hydrogens H_3 and H_7 can be clearly observed, confirming the ligand double deprotonation, as well as the shifting of all the signals due to nickel coordination.

The ^{13}C NMR spectra of the ligands also agree with their structures. In the complexes, as in the IR spectra, the signals of the C=N groups are shifted, indicating their coordination to nickel. Conversely, the signals corresponding to the C=S groups hardly move; however, this does not indicate that the sulfurs do not coordinate the metal, but that the electronic delocalization in the ligand after deprotonation and the ability of the sulfur to accept electron density by back-donation, ensure that the electronic environment of the sulfur does not change before and after coordination, which does not rule out the tetradentate coordination of the ligands, as it is its common behaviour, and is strongly supported by the strong preference of nickel(II) to form square-planar complexes.

2.4. Crystal Structures

The crystal structure of the triazine obtained as a by-product in the synthesis of HAClPhTs was solved by single crystal X-ray diffraction (Figure 1, complete data can be found in Supplementary Materials). Crystal data for $C_{13}H_{16}ClN_3OS$ (M = 297.80 g/mol) were: monoclinic, space group $P_{21/n}$, a = 8.5444(2) Å, b = 17.0578(4) Å, c = 10.2898(2) Å, β = 96.1840(10)°, V = 1491.00(6) Å^3, Z = 4, T = 296(2) K, μ(MoKα) = 0.71073 mm^{-1}, D_{calc} = 1.327 g/cm^3, 22,946 reflections measured (2.321° ≤ 2Θ ≤ 26.403°), 3042 unique (Rint = 0.0288), which were used in all calculations. The final R1 was 0.0403 (I > 2σ(I)) and wR2 was 0.1327 (all data).

This compound is formed by subsequent cyclization of the monoketone by condensation of the NH_2 group with the C=O group. As there is a pendant group in the nitrogen, an imine bond cannot be formed and an ethoxide group is inserted into the carbon leading to *sp*^{3} hybridization that ensures that the ring is not planar. This carbon is chiral and the compound is obtained as the R isomer. The C-S bond distance is 1.682(2), so the molecule is

the thione tautomeric form with the proton in the hydrazinic nitrogen. The chlorophenyl ring is almost perpendicular to the triazine, forming an angle of 81.25°.

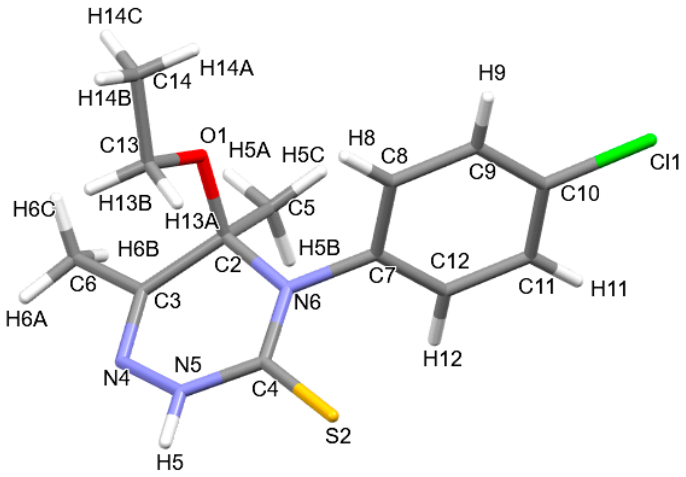

Figure 1. Molecular structure of the 1,2,4-triazine-3-thione.

2.5. Photocatalytic Degradation of MO

The photocatalytic activity of the three complexes in the degradation of methyl orange was studied. In a previous work, we published the photocatalytic activity of other nickel and zinc complexes, in which we used a ratio mg of catalyst versus mL of substrate of 2:1. As this catalyst/substrate ratio is high, the first thing we did was to evaluate whether we could obtain similar results by decreasing the amount of catalyst. Ratios of 2:1, 1:1, 0.5:1 and 0.25:1 were tested, and the results show that using 0.5 mg of catalyst per mL of MO solution yields the same results as with larger ratios, but that below this ratio, the photocatalytic activity decreases. Therefore, for the rest of the tests, the proportion 0.5:1 was used. To check the integrity of the catalyst after photocatalysis, IR and ^{1}H NMR spectra were carried out, and in all cases, it was observed that these coincide with those of the complexes used.

Figure 2 illustrates the photoactivity of nickel complexes **1**–**3** under UV–vis irradiation. As observed, they effectively degrade the organic dye, albeit with some differences. Complex **1** showed the least degradation of MO. Complex **2** exhibited the highest photocatalytic activity for methyl orange degradation, followed by complex **3**. Notably, complex **2** achieved maximum degradation within 24 h, whereas complex **3** required 72 h to reach similar degradation levels (Figure 2d,e). These results shows that the photoactivity of these complexes is much higher than for other nickel(II) complexes with bis(thiosemicarbazone) ligands reported by our group, which only degrade the 5% of MO in 24 h [30], confirming the decisive role that the ligands play in the photocatalytic activity.

If we look at the time in which the degradation of half of the initial concentration of MO is reached (Figure 2e), we can observe the following order of kinetic rates: complex **2** > complex **3** > complex **1**. Based on these results, some general tendencies can be observed: the complexes with the ligand bearing a 4-chlorophenyl substituent are the ones that present better photodegradation rates of methyl orange. In contrast, the nickel complex with naphthalene **1** is the least efficient.

The degradation of methyl orange by nickel(II) thiosemicabazonate complexes is an interesting process involving several chemical reactions. A general explanation of the process is given: nickel complexes act as photocatalysts under light irradiation. The light excites the electrons in the complex, promoting the formation of electron–hole pairs. The electron–hole pairs generated can react with water and oxygen present in the solution to form hydroxyl (•OH) and superoxide ($O_2^{\bullet -}$) radicals. These radicals are highly reactive and can attack methyl orange molecules. The hydroxyl and superoxide radicals oxidize the

methyl orange molecules, breaking the azo bonds and degrading the dye into simpler, less toxic products. This oxidation–reduction process is key to the effective degradation of the dye. Nickel thiosemicarbazone complexes can also directly interact with methyl orange molecules, facilitating electron transfer and improving the efficiency of the degradation process, and it is here that the presence of different substituents can enhance this interaction. This mechanism is similar to that observed in other heterogeneous photocatalytic processes, where metal catalysts play a crucial role in the generation of reactive species and in the degradation of organic pollutants.

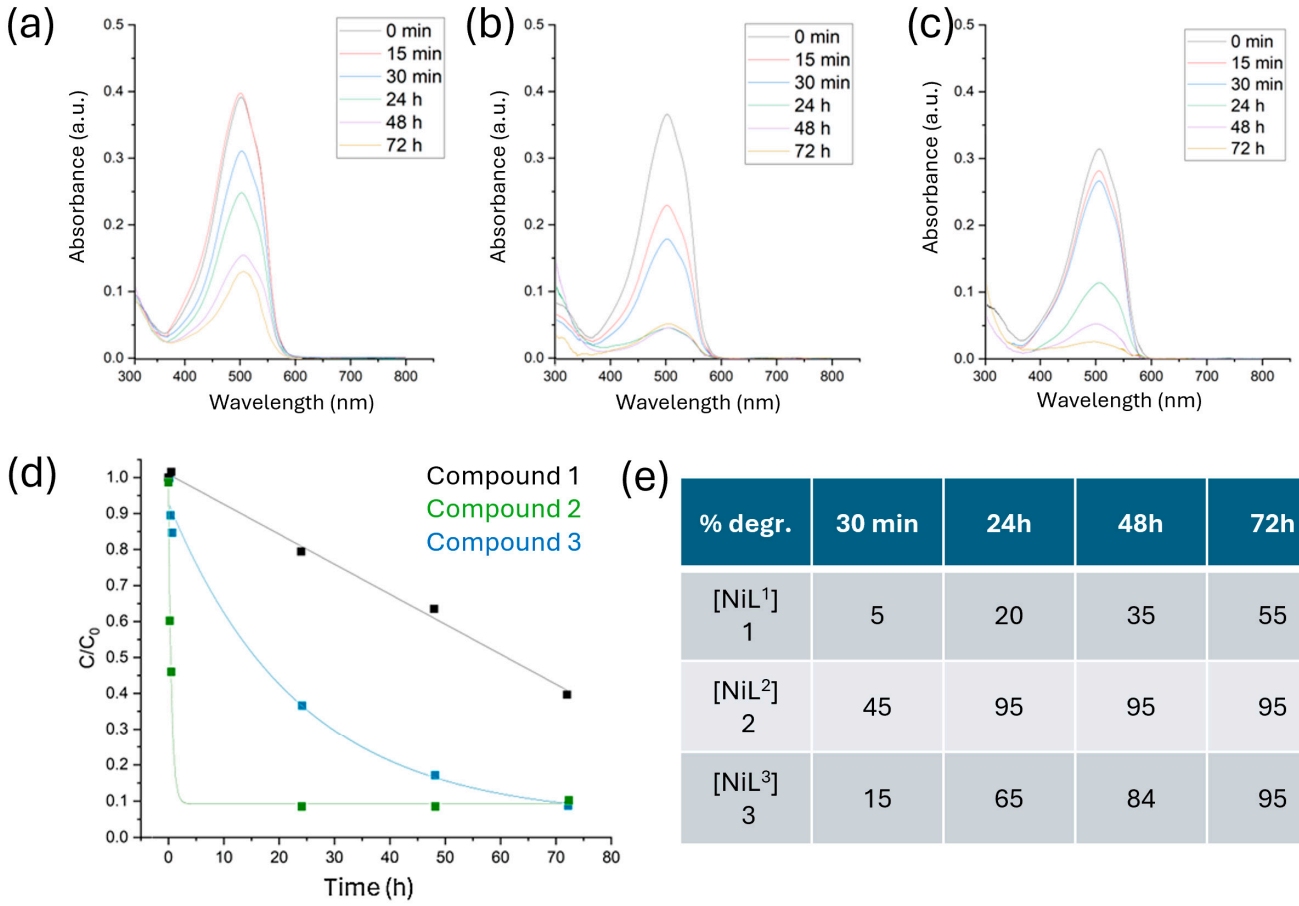

(e)

% degr.	30 min	24h	48h	72h
[NiL^1] 1	5	20	35	55
[NiL^2] 2	45	95	95	95
[NiL^3] 3	15	65	84	95

Figure 2. UV–vis spectra and evolution of the MO concentration with the reaction time for the complexes: (**a**) complex **1**, (**b**) complex **2** and (**c**) complex **3**, (**d**) kinetic of the MO degradation for the three complexes, and (**e**) table with the % of degradation with time.

2.6. Theoretical Calculations

To explore the observed trend, computational calculations were conducted. The results align with the experimental findings, indicating that the complexes exhibit a HOMO–LUMO gap (Figure 3, Table 1) in the following order: complex **1** > complex **2** > complex **3**. Notably, complex **2**, which demonstrates the best degradation kinetics, has a HOMO–LUMO gap of 1.492 eV. It is known that the interval between the highest occupied molecular orbital (HOMO) and the lowest unoccupied molecular orbital (LUMO) is a crucial factor influencing the chemical reactivity and efficiency of photodegradation processes. A smaller HOMO–LUMO interval generally indicates higher reactivity, as it facilitates electron transfer during photocatalytic excitation [31].

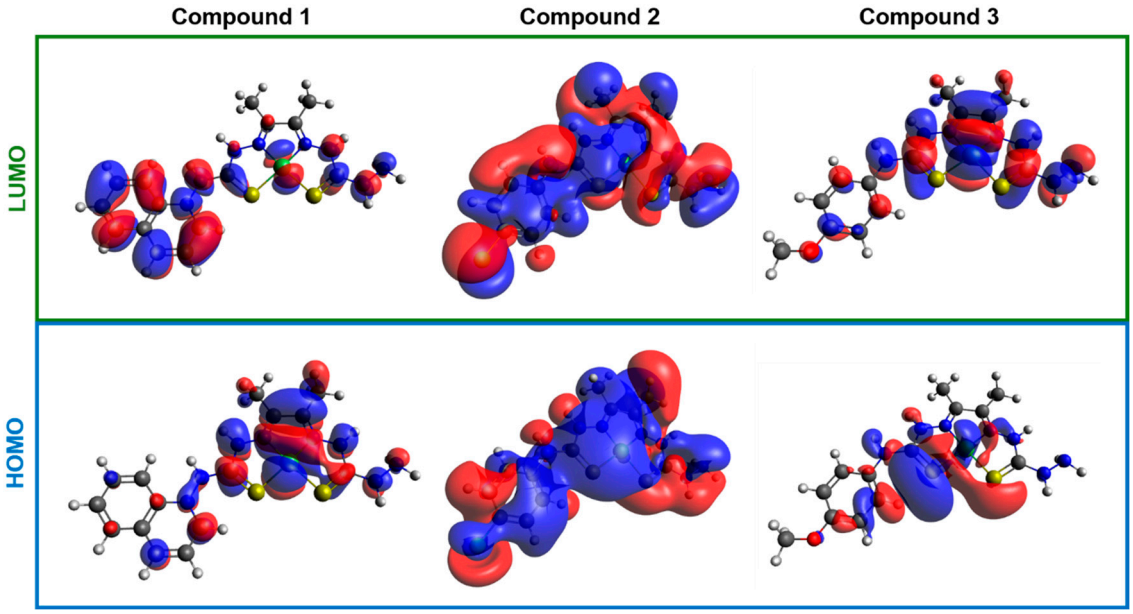

Figure 3. Frontier molecular orbitals for complexes **1**–**3**.

Table 1. Molecular orbital (MO) composition and energy values of the HOMO, LUMO, HOMO–LUMO (H–L) gaps. All the energies are reported in eV.

Complex	E_{HOMO}	MO Composition	E_{LUMO}	MO Composition	H–L Gap
1	−9.061	75% ligand 25% Ni	−3.354	95% ligand 5% Ni	5.707
2	−3.924	50% ligand 50% Ni	−2.432	50% ligand 50% Ni	1.492
3	−3.237	85% ligand 15% Ni	−2.265	50% ligand 50% Ni	0.972

In the case of nickel thiosemicarbazone complexes, the photodegradation of methyl orange is affected by the ability of the complex to absorb light and generate electron–hole pairs. Reducing the HOMO–LUMO interval in these complexes improves the efficiency of photodegradation by allowing greater light absorption and more efficient electron transfer [31,32].

As can be seen, the complex with the largest gap (5.707 eV), complex **1**, shows the lowest activity, followed by complex **3**, which shows the smallest gap value (0.972 eV). Complex **2**, with a gap value of 1.492 eV, showed the best photoactivity, which confirms that it has both adequate energy levels of HOMO and LUMO, as well as a gap value between the two suitable to make the most of the light photons and produce photodegradation. This may explain its significantly faster degradation of methyl orange, taking about four times less time than complex **3**, the second most photoactive complex. Overall, these findings suggest that optimal HOMO and LUMO energy levels, along with a HOMO–LUMO energy difference of approximately 1.5 eV, are crucial for effective photodegradation of methyl orange.

2.7. Photocatalytic Water Splitting

We studied the photocatalytic activity of the nickel complexes in promoting water splitting. The amount of H_2 evolved in the reaction was measured by gas chromatography. The results show that the three complexes can photocatalyze the water splitting in the reaction conditions tested (11 mL of water/methanol 1:1, 11 mg of the complex, 30 min of irradiation). In these conditions, complex **1** produces 0.22 μmol h^{-1} g^{-1}, complex **2** 3.96 μmol h^{-1} g^{-1} and complex **3** 11.6 μmol h^{-1} g^{-1}. If we compare these values with

the ones obtained for the analogous complexes containing thiosemicarbazide instead of thiocarbohydrazide [28], we can see the amount of hydrogen evolved is smaller (from 2.61 to 30.63 μmol h^{-1} g^{-1} in the same conditions), although the three complexes can promote water splitting. Therefore, the introduction of a hydrazinic nitrogen in the ligand skeleton does not improve water splitting but rather worsen the photocatalytic performance. Nevertheless, the results are promising since the three nickel complexes studied evolve hydrogen in equivalent amounts to other reported symmetrical bis(thiosemicarbazone) complexes used together with a sacrificial electron donor and a photosensitizer [33], which again seems to be related to the asymmetry of the ligands.

3. Experimental Section

All the chemicals were purchased from standard commercial sources and used as received. Microanalyses were carried out using a LECO CHNS-932 Elemental Analyzer, (LECO Corporation, USA). IR spectra in the 4000–400 cm^{-1} range were recorded as KBr pellets on a Jasco FT/IR-410 spectrophotometer, JASCO, Japan. The ESI mass spectra in positive mode were recorded on a Q-STAR PULSAR I (Applied Biosystems, UK) instrument using a hybrid analyzer QTOF (Quadrupole time-of-flight). ^{1}H and ^{13}C NMR spectra were recorded on a spectrometer Bruker AVIII HD-300 MHz (Bruker, USA) using DMSO-d_6 as solvent and TMS as reference. UV-Vis spectra were recorded on a VWR UV-6300PC spectrophotometer (VWR, USA) using solutions 10^{-3} and 10^{-5} M in DMF.

3.1. Synthesis of the Organic Compounds

The atom labeling used for spectra assignments is in Scheme 3.

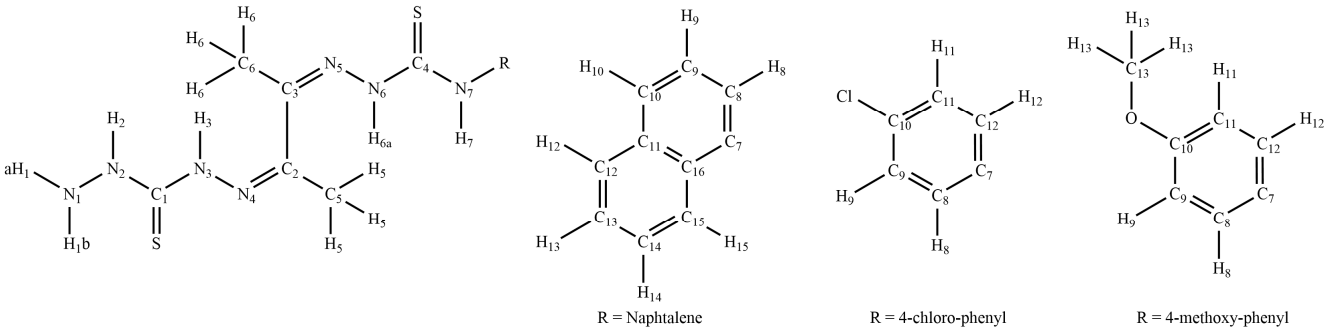

Scheme 3. Atom labeling used for the spectra assignment.

4-(1-naphthyl)-3-thiosemicarbazide, *4-(4-chlorophenyl)-3-thiosemicarbazide* and *4-(4-methoxyphenyl)*-3-thiosemicarbazide were synthesized according to the procedure previously reported [24,25].

HANfTs, HAClPhTs and HAOMePhTs were synthesized using the previously reported procedure for the obtaining of other 2,3-butanedione monoketones [24,25,28,29], in which one equivalent of the corresponding thiosemicarbazide is reacted with three equivalents of 2,3-butanedione in water at room temperature for one hour.

Diacetyl-2-(1-naphthyl-3-thiosemicarbazone), HANfTs. Yield 86%. Anal. calcd. for $C_{15}H_{15}N_3SO$ (MW 285.34) (%): C, 63.13; H, 5.30; N, 14.73; S, 11.24. Found (%): C, 63.37; H, 5.14; N, 14.55 S, 11.03. IR (KBr) ν/cm^{-1}: 3342, 3273 (NH), 1685 (C=O), 1598 (C=N), 1512, 1488 (thioamide I, CC_{ar}), 841 (thioamide IV), 808, 760 (CH_{oop}). ^{1}H NMR (300 MHz, DMSO-d_6) δ (ppm): 11.07 (1H, s, H_{6a}), 10.48 (1H, s, H_7), 8.02–7.99 (1H, dd, H_{15}), 7.88–7.84 (1H, m, H_{10}), 7.61–7.54 (4H, m, H_8+H_9+H_{13}+H_{14}), 2.51 (3H, s, H_5), 2.09 (3H, s, H_6).

Diacetyl-2-(4-chlorophenyl-3-thiosemicarbazone), HAClPhTs. Yield 94%. Anal. calcd. for $C_{11}H_{12}N_3SO$ (MW 234.28) (%): C, 56.39; H, 5.16; N, 17.94; S, 13.68. Found (%): C, 56.64; H, 5.21; N, 17.74; S, 13.51. IR (KBr) ν/cm^{-1}: 3263, 3194 (NH), 1690 (C=O), 1605 (C=N), 1584,

1523, 1489 (thioamide I, CC_{ar}), 929 (thioamide IV), 834, 796 (CH_{oop}). ^{1}H NMR (300 MHz, DMSO-d_6) δ (ppm): 11.07 (1H, s, H_7), 10.22 (1H, s, H_{6a}), 7.61 (2H, d, ^3J = 8.8, H_8+H_{12}), 7.47 (2H, d, ^3J = 8.8, H_9+H_{11}), 2.49 (3H, s, H_5), 2.04 (3H, s, H_6).

Diacetyl-2-(4-methoxyhenyl-3-thiosemicarbazone), HAOMePhTs. Yield 89%. Anal. calcd. for $C_{11}H_{12}N_3SO$ (MW 256.31) (%): C, 54.32; H, 5.70; N, 15.82; S, 12.08. Found (%): C, 54.57; H, 5.94; N, 15.74 S, 11.93. IR (KBr) ν/cm^{-1}: 3308, 3170 (NH), 1687 (C=O), 1590 (C=N), 1608, 1521, 1488 (thioamide I, CC_{ar}), 926 (thioamide IV), 830, 814 (CH_{oop}). ^{1}H NMR (300 MHz, DMSO-d_6) δ (ppm): 10.88 (1H, s, H_7), 10.09 (1H, s, H_{6a}), 7.40 (2H, d, ^3J = 8.8, H_8+H_{12}), 6.96 (2H, d, ^3J = 8.8, H_9+H_{11}), 3.78 (3H, s, H_{13}), 2.48 (3H, s, H_5), 2.03 (3H, s, H_6).

The dissymmetric ligands were obtained following the same procedure: a suspension of 0.150 g (1.6 mmol) of thiocarbohydrazide in 15 mL of ethanol was heated at 50 °C. Thereafter, 1.6 mmol of the corresponding solid monoketone and one drop of 7% HCl were added, and the mixture was refluxed for 3 h. The pale-yellow solid was filtered, washed with ethanol and dried on filter paper.

Diacetyl-2-(1-naphthyl-3-thiosemicarbazone),3-(thiocarbohydrazone), $\boldsymbol{L^1H_2}$. Yield 89%. Anal. calcd. for $C_{16}H_{19}N_7S_2$ (MW 373.46) (%): C, 51.45; H, 5.13; N, 26.25; S, 17.17. Found (%): C, 51.62; H, 5.25; N, 26.35; S, 17.11. IR (KBr) ν/cm^{-1}: 3326, 3283, 3260, 3238, 3182 (NH), 1597 (C=N), 1494 (thioamide I, CC_{ar}), 824 (thioamide IV), 789, 771 (CH_{oop}). ^{1}H NMR (300 MHz, DMSO-d_6) δ (ppm): 10.68 (1H, s, H_{6a}), 10.24 (2H, s, H_3 + H_7), 9.76 (1H, s, H_2), 8.02–7.96 (1H, m, H_{12}), 7.94–7.89 (1H, m, H_{13}), 7.87–7.82 (1H, m, H_{10}),7.60–7.52 (4H, m, H_8+H_9+H_{14}+H_{15}), 5.03 (2H, s, H_{1a}+H_{1b}), 2.33, (3H, s, H_5), 2.27 (3H, s, H_6). ^{13}C NMR (75 MHz, DMSO-d_6) δ (ppm): 179.2, (C_1), 176.4 (C_4), 149.9, 149.0 (C_2, C_3), 136.1 (C_7), 134.2 (C_{11}), 130.8 (C_{16}), 128.6 (C_9), 127.4 (C_{15}), 126.7 (C_{14}), 126.6 (C_{12}), 126.5 (C_{13}), 125.9 (C_{10}), 123.6 (C_8), 12.4, 12.3 (C_5, C_6). UV–visible spectrum (DMF), λ_{max} (nm), (ε, Lmol^{-1}cm^{-1}): 340 (57,320), 447 (5,730).

Diacetyl-2-(4-chlorophenyl-3-thiosemicarbazone)-3-(thiocarbohydrazone), $\boldsymbol{L^2H_2}$. Yield 87%. Anal. calcd. for $C_{12}H_{16}N_7S_2Cl$ (MW 357.85) (%): C, 40.27; H, 4.51; N, 27.40; S, 17.92. Found (%): C, 40.47; H, 4.60; N, 27.65; S, 17.85. IR (KBr) ν/cm^{-1}: 3340, 3303, 3254, 3165 (NH), 1590 (C=N), 1497 (thioamide I, CC_{ar}), 925 (thioamide IV), 825, 771 (CH_{oop}). ^{1}H NMR (300 MHz, DMSO-d_6) δ (ppm): 10.66 (1H, s, H_7), 10.27 (1H, s, H_3), 9.97 (1H, s, H_{6a}), 9.73 (1H, s, H_2), 7.61 (2H, m, H_8+H_{12}), 7.47 (2H, m, H_9+H_{11}), 4.98 (2H, s, H_{1a}+H_{1b}), 2.27 (3H, s, H_5), 2.24 (3H, s, H_6). ^{13}C NMR (75 MHz, DMSO-d_6) δ (ppm): 177.3, 176.4 (C_1, C_4), 150.3, 146.1 (C_2, C_3), 138.5 (C_7), 133.2 (C_{10}), 128.5 (C_9+C_{11}), 127.8 (C_8+C_{12}), 12.5, 12.2 (C_5, C_6). UV–visible spectrum (DMF), λ_{max} (nm), (ε, Lmol^{-1}cm^{-1}): 341 (71,710), 423 (3086).

Diacetyl-2-(4-methoxyphenyl-3-thiosemicarbazone)-3-(thiocarbohydrazone), $\boldsymbol{L^3H_2}$. Yield 84%. Anal. calcd. for $C_{13}H_{19}N_7S_2O$ (MW 353.43) (%): C, 44.17; H, 5.42; N, 27.74; S, 18.14. Found (%): C, 44.35; H, 5.63; N, 27.58; S, 17.99. IR (KBr) ν/cm^{-1}: 3288, 3260, 3217, 3176 (NH), 1594 (C=N), 1492 (thioamide I, CC_{ar}), 934 (thioamide IV), 829, 811 (CH_{oop}). ^{1}H NMR (300 MHz, DMSO-d_6) δ (ppm): 10.46 (1H, s, H_7), 10.25 (1H, s, H_3), 9.83 (1H, s, H_{6a}), 9.72 (1H, s, H_2), 7.41 (2H, m, H_9+H_{11}), 6.94 (2H, m, H_8+H_{12}), 4.98 (2H, s, H_{1a}+H_{1b}), 3.77 (3H, s, H_{13}), 2.26 (3H, s, H_5), 2.23 (3H, s, H_6). ^{13}C NMR (75 MHz, DMSO-d_6) δ (ppm): 177.6, 176.4 (C_1, C_4), 157.5 (C_{10}), 149.6, 148,8 (C_2,C_3), 132.4 (C_7), 127.8 (C_9+C_{11}), 113.8 (C_8+C_{12}), 55.7 (C_{13}), 12.4, 12.2 (C_5, C_6). UV-visible spectrum (DMF), λ_{max} (nm), (ε, Lmol^{-1}cm^{-1}): 384 (74,590), 429 (3,960).

3.2. Synthesis of the Coordination Compounds

The three nickel complexes were synthesized using the same procedure in which 0.27 mmol of nickel(II) nitrate hexahydrate was dissolved in 1 mL of ethanol and added to a suspension of the corresponding ligand (0.27 mmol) in 5 mL of the same solvent.

The mixture was heated under reflux for 2 h and the brown solid was filtered, washed thoroughly with water and dried on air.

[NiL^1], **1**. Yield 94%. Anal. calcd. for $NiC_{16}H_{17}N_7S_2$ (MW 430.14) (%): C, 44.67; H, 3.98; N, 22.79; S, 14.91. Found (%): C, 44.43; H, 4.18; N, 22.62; S, 14.76. ESI-MS m/z: 430.04 $[M+H]^+$, 859.07 $[2M+H]^+$. IR (KBr) ν/cm^{-1}: 3387, 3316, 3192 (NH), 1596 (C=N), 1562, 1540, 1473 (thioamide I, CC_{ar}), 832 (thioamide IV), 789, 771 (CH_{oop}). ^{1}H NMR (300 MHz, DMSO-d_6) δ (ppm): 10.24 (1H, s, H_7), 10.06 (1H, s, H_2), 7.97–7.90 (2H, m, H_{12}+H_{13}), 7.89–7.77 (1H, m, H_{10}), 7.60–7.45 (4H, m, H_8+H_9+H_{14}+H_{15}), 3.45 (2H, br s, H_{1a}+H_{1b}), 2.02, (3H, s, H_5), 1.86 (3H, s, H_6). ^{13}C NMR (75 MHz, DMSO-d_6) δ (ppm): 178.6, (C_1), 176.4 (C_4), 161.9, 157.9 (C_2, C_3), 136.1 (C_7), 134.0 (C_{11}), 130.8 (C_{16}), 129.2 (C_9), 128.5 (C_{15}), 126.8 (C_{14}), 126.7 (C_{12}), 125.8 (C_{13}), 124.4 (C_{10}), 123.5 (C_8), 14.8, 14.6 (C_5, C_6). UV-visible spectrum (DMF), λ_{max} (nm), (ε, $Lmol^{-1}cm^{-1}$): 262 (61,450), 450 (20,100), 680 (632).

[NiL^2], **2**. Yield 94%. Anal. calcd. for $NiC_{12}H_{14}N_7S_2Cl$ (MW 414.52) (%): C, 34.77; H, 3.40; N, 23.65; S, 15.47. Found (%): C, 34.96; H, 3.65; N, 23.40; S, 15.34. ESI-MS *m/z*: 413.99 $[M+H]^+$, 826.97 $[2M+H]^+$. IR (KBr) ν/cm^{-1}: 3301, 3186, 3121 (NH), 1598 (C=N), 1543, 1511, 1489, 1472 (thioamide I, CC_{ar}), 867 (thioamide IV), 822 (CH_{oop}). ^{1}H NMR (300 MHz, DMSO-d_6) δ (ppm): 10.17 (2H, s, H_2 + H_7), 7.62 (2H, d, ^3J = 9.0, H_8 + H_{12}), 7.36 (2H, d, ^3J = 9.0, H_9 + H_{11}), 2.07 (3H, s, H_5), 2.06 (3H, s, H_6). ^{13}C NMR (75 MHz, DMSO-d_6) δ (ppm): 176.6, 173.7 (C_1, C_4), 161.8, 160.7 (C_2,C_3), 139.5 (C_7), 129.04 (C_{10}), 127.3 (C_9 + C_{11}), 121.8 (C_8 + C_{12}), 15.3, 14.8 (C_5, C_6). UV-visible spectrum (DMF), λ_{max} (nm), (ε, $Lmol^{-1}cm^{-1}$): 264 (11,980), 445 (50,940), 690 (536).

[NiL^3], **3**. Yield 94%. Anal. calcd. for $NiC_{13}H_{17}N_7S_2O$ (MW 410.14) (%): C, 38.07; H, 4.18; N, 23.91; S, 15.63. Found (%): C, 37.76; H, 3.98; N, 24.04; S, 15.45. ESI-MS *m/z*: 410.04 $[M+H]^+$, 819.07 $[2M+H]^+$. IR (KBr) ν/cm^{-1}: 3305, 3196, 3130 (NH), 1605 (C=N), 1549, 1508, 1477 (thioamide I, CC_{ar}), 970 (thioamide IV), 837, 823 (CH_{oop}). ^{1}H NMR (300 MHz, DMSO-d_6) δ (ppm): 10.16 (1H, s, H_7), 10.01 (1H, s, H_2), 7.89 (2H, m, H_9 + H_{11}), 7.51 (2H, m, H_8 + H_{12}), 3.72 (3H, s, H_{13}), 3.43 (2H, br s, H_{1a} + H_{1b}), 2.06 (3H, s, H_5), 2.05 (3H, s, H_6). ^{13}C NMR (75 MHz, DMSO-d_6) δ (ppm): 176.3 (C_1, C_4), 161.9 (C_{10}), 158.6, 155.8 (C_2,C_3), 133.9 (C_7), 122.0 (C_9 + C_{11}), 114.3 (C_8 + C_{12}), 55.6 (C_{13}), 15.0, 14.8 (C_5, C_6). UV-visible spectrum (DMF), λ_{max} (nm), (ε, $Lmol^{-1}cm^{-1}$): 265 (136,300), 450 (58,230), 685 (623).

3.3. Computational Studies

All calculations were carried out using the Gamess program [34]. The computational models were built by considering the X-ray diffraction single crystal data of previous similar compounds reported in the group [29], and the structures optimized by molecular mechanics calculations, in particular, UFF using the Avogadro 1.2.0 program [35]. The afore-mentioned models were fully optimized at the scalar relativistic DFT level using the B3LYP—RHF approximation with the LANL2DZ basis set. This methodology was validated based on structural determinations between crystallographic and experimental section data in a previous work published by the group [30].

3.4. Testing of the Photocatalytic Activity for the Degradation of Methyl Orange

The photocatalytic activity of the three complexes in degrading methyl orange (MO) was evaluated by preparing a suspension of the complex (5 mg) in an aqueous solution of methyl orange (10^{-5} M, 10 mL) in a sealed vial. The mixture was stirred while being irradiated with a high-pressure mercury vapor lamp (250 W, HPL-N Philips, Amsterdam, The Netherlands). Aliquots of 1 mL were taken with a syringe at different irradiation times, and their absorption spectra were recorded using a spectrophotometer. The concentration of methyl orange was determined by analyzing the changes in absorbance at 465 nm. In cases where the MO signal overlapped with other signals, the spectra were deconvoluted to

unambiguously assign the intensity of the methyl orange absorption maximum to the MO concentration. To account for potential side effects that could decrease the MO concentration, two additional factors were considered during data analysis: the self-degradation of MO under UV-vis irradiation and its degradation in the absence of light (non-photocatalytic degradation). Therefore, two additional experiments were conducted: a solution of MO without any complex was irradiated under the same experimental conditions, resulting in no degradation of MO. Additionally, suspensions of MO with the different complexes were prepared as described above but kept in the dark, showing no changes in MO concentration, thus ruling out non-photocatalytic degradation. The experiments were repeated three times, with all cases showing a statistical uncertainty below 1%.

3.5. Testing of the Photocatalytic Activity for Water Splitting

The photocatalytic activity of the nickel complexes was evaluated by preparing a suspension of 11 mg of the complex in a mixture of 5.5 mL of water and 5.5 mL of methanol in a sealed vial. The reaction mixture was purged with N_2 for 10 min in dark conditions, followed by irradiation for 30 min using a 300 W Xe lamp positioned in front of the sealed vial. Gas samples of 1 mL were taken from the headspace and immediately injected into a gas chromatograph (Agilent GC 8860) equipped with HP-PLOT-Q/HP-PLOT-mole sieve 5Å columns (0.53/0.32 mm I.D. 30 m) and TCD/FID detectors for the quantification of inert gases (H_2, O_2, N_2) and organic substances. The reported results are the average of three independent experiments, with control experiments performed under the same conditions but without the catalyst.

3.6. Crystallographic Data and Structure Determination

Crystallographic data were collected on a Bruker Kappa Apex II diffractometer equipped with an Apex-II CCD area detector using a graphite monochromator (Mo k_α radiation, λ = 0.71073 Å). CCDC number 2405702 contains supplementary crystallographic data for this paper. These data can be obtained free of charge via http://www.ccdc.cam.ac.uk, or from the Cambridge Crystallographic Data Centre, 12 Union Road, Cambridge, CB2 1EZ, UK; fax: (+44) 1223-336-033; or e-mail: deposit@ccdc.cam.ac.uk.

4. Conclusions

We have synthesized three new unsymmetrical ligands based on different thiosemicarbazones, as well as their nickel(II) complexes. The potential use of the complexes to act as a photocatalyst in the degradation of methyl orange has been tested and the results show that they can effectively degrade the pollutant. Compared to previous results, it seems that the introduction in the ligand backbone of an additional hydrazinic NH group favors the catalytic performance of the complexes. Theoretical calculations show that the photocatalytic activity depends on the HOMO–LUMO gap, which depends on the substituent attached to the terminal NH group in the ligand skeleton. A test was also performed to check if the complexes can also photocatalyze HER, and the results indicate that they can produce molecular hydrogen, although a deeper study must be made to optimize the photocatalytic activity.

Supplementary Materials: The following supporting information can be downloaded at: https://www.mdpi.com/article/10.3390/inorganics13020040/s1. It includes mass spectra of the complexes and IR, UV-Vis, ^{1}H and ^{13}C NMR spectra of the ligands and the complexes.

Author Contributions: Conceptualization, E.L.-T. and M.A.M.; investigation, R.B.; data curation, D.G.C.; writing—review and editing, E.L.-T. and D.G.C.; supervision, E.L.-T. All authors have read and agreed to the published version of the manuscript.

Funding: This research was funded by grant TED2021-129876B-I00 of the Ministerio de Ciencia, Innovación y Universidades (Spain).

Data Availability Statement: Crystallographic data can be obtained free of charge via http://www.ccdc.cam.ac.uk, or from the Cambridge Crystallographic Data Centre, 12 Union Road, Cambridge, CB2 1EZ, UK; fax: (+44)-1223-336-033; or e-mail: deposit@ccdc.cam.ac.uk.

Conflicts of Interest: The authors declare no conflict of interest.

References

1. WHO. Drinking-Water, (n.d.). Available online: https://www.who.int/news-room/fact-sheets/detail/drinking-water (accessed on 18 December 2024).
2. Akika, F.Z.; Rouibah, K.; Benamira, M.; Avramova, I. Elaboration of the new heterostructure of $NiAl_2O_4$/kaolin and its photocatalytic activity towards methyl green under solar light irradiation. *Inorg. Chem. Commun.* **2023**, *154*, 110878. [CrossRef]
3. Tkaczyk, A.; Mitrowska, K.; Posyniak, A. Synthetic organic dyes as contaminants of the aquatic environment and their implications for ecosystems: A review. *Sci. Total Environ.* **2020**, *714*, 137222. [CrossRef]
4. Matsuyama, K.; Kawahara, Y.; Shoji, A.; Kato, T.; Okuyama, T. Supercritical CO_2-assisted formation of metal-organic framework-loaded porous polystyrene membranes for dye removal. *J. Appl. Polym. Sci.* **2023**, e54347. [CrossRef]
5. Badawi, A.K.; Salama, R.S.; Mostafa, M.M.M. Natural-based coagulants/flocculants as sustainable market-valued products for industrial wastewater treatment: A review of recent developments. *RSC Adv.* **2023**, *13*, 19335. [CrossRef] [PubMed]
6. Ahmadipouya, S.; Mousavi, S.A.; Shokrgozar, A.; Mousavi, D.V. Improving dye removal and antifouling performance of polysulfone nanofiltration membranes by incorporation of UiO-66 metal-organic framework. *J. Environ. Chem. Eng.* **2022**, *10*, 107535. [CrossRef]
7. Barragán, B.E.; Costa, C.; Márquez, M.C. Biodegradation of azo dyes by bacteria inoculated on solid media. *Dyes Pigment.* **2007**, *75*, 73. [CrossRef]
8. Au, V.K.-M.; Kwan, S.Y.; Lai, M.N.; Low, K.-H. Dual-functional mesoporous copper(II) metal-organic frameworks for the remediation of organic dyes. *Chem. Eur. J.* **2021**, *27*, 9174. [CrossRef] [PubMed]
9. Rizala, M.Y.; Saleha, R.; Taufik, A. Characterization and photocatalytic activity of Ag/Mn_3O_4/graphene composites under visible light irradiation for organic dyes degradation. *J. Environ. Chem. Eng.* **2020**, *8*, 103610. [CrossRef]
10. Comparelli, R.; Fanizza, E.; Curri, M.L.; Cozzoli, P.D.; Mascolo, G.; Passino, R.; Agostiano, A. UV-induced photocatalytic degradation of azo dyes by organic-capped ZnO nanocrystals immobilized onto substrates. *Appl. Catal. B-Environ.* **2005**, *55*, 81. [CrossRef]
11. Carvalho, S.S.F.; Rodrigues, A.C.C.; Lima, J.F.; Carvalho, N.M.F. Photocatalytic degradation of dyes by mononuclear copper(II) complexes from bis-(2-pyridylmethyl)amine NNN-derivative ligands. *Inorg. Chim. Acta* **2020**, *512*, 119924. [CrossRef]
12. Jennifer, S.J.; Jana, A.K. Influence of pyrazine/piperazine based guest molecules in the crystal structures of uranyl thiophene dicarboxylate coordination polymers: Structural diversities and photocatalytic activities for the degradation of organic dye. *Cryst. Growth Des.* **2017**, *17*, 5318. [CrossRef]
13. Ghosh, K.; Harms, K.; Franconetti, A.; Frontera, A.; Chattopadhyay, S. A triple alkoxo bridged dinuclear cobalt(III) complex mimicking phosphatase and showing ability to degrade organic dye contaminants by photocatalysis. *J. Organomet. Chem.* **2019**, *883*, 52. [CrossRef]
14. Bajaj, K.; Buchanan, R.M.; Grapperhaus, C.A. Antifungal activity of thiosemicarbazones, bis(thiosemicarbazones), and their metal complexes. *J. Inorg. Biochem.* **2021**, *225*, 111620. [CrossRef] [PubMed]
15. Miglioli, F.; De Franco, M.; Bartoli, J.; Scaccaglia, M.; Pelosi, G.; Marzano, C.; Rogolino, D.; Gandin, V.; Carcelli, M. Anticancer activity of new water-soluble sulfonated thiosemicarbazone copper(II) complexes targeting disulfide isomerase. *Eur. J. Inorg. Chem.* **2024**, *276*, 116697. [CrossRef] [PubMed]
16. Gómez, E.; Galván-Hidalgo, J.M.; Pérez-Cuéllar, G.; Huerta-Landa, K.A.; González-Hernández, A.; Gómez-García, O.; Andrade-Pavón, D.; Ramírez-Apan, T.; Hernández, K.D.R.; Hernández, S.; et al. New Organotin (IV) compounds derived from dehydroacetic acid and thiosemicarbazides: Synthesis, rational design, cytotoxic evaluation, and molecular docking simulation. *Bioinorg. Chem. Appl.* **2023**, *2023*, 901843. [CrossRef] [PubMed]
17. Parrilha, G.L.; Santos, R.G.D.; Beraldo, H. Applications of radiocomplexes with thiosemicarbazones and bis(thiosemicarbazones) in diagnostic and therapeutic nuclear medicine. *Coord. Chem. Rev.* **2022**, *458*, 214418. [CrossRef]
18. Murugan, K.; Vijayapritha, S.; Viswanathamurthi, P.; Saravanan, K.; Vijayan, P.; Ojwach, S.O. Ru (II) complexes containing (2-(pyren-1-ylmethylene) hydrazinyl) benzothiazole: Synthesis, solid-state structure, computational study and catalysis in N-alkylation reactions. *Inorg. Chim. Acta* **2020**, *512*, 119864. [CrossRef]

19. Ravindran, A.; Sindhuja, D.; Bhuvanesh, N.; Karvembu, R. Synthesis of 1, 2-Disubstituted Benzimidazoles via Acceptorless Dehydrogenative Coupling Using Ru (II)-Arene Catalysts Containing Ferrocene Thiosemicarbazone. *Eur. J. Inorg. Chem.* **2022**, *2022*, e202200181. [CrossRef]
20. Haddad, A.Z.; Cronin, S.P.; Mashuta, M.S.; Buchanan, R.M.; Grapperhaus, C.A. Metal-assisted ligand-centered electrocatalytic hydrogen evolution upon reduction of a bis(thiosemicarbazonato)Cu(II) complex. *Inorg. Chem.* **2017**, *56*, 11254. [CrossRef] [PubMed]
21. Straistari, T.; Hardré, R.; Fize, J.; Shova, S.; Giorgi, M.; Réglier, M.; Artero, V.; Orio, M. Hydrogen evolution reactions catalyzed by a bis(thiosemicarbazone) cobalt complex: An experimental and theoretical study. *Chem. Eur. J.* **2018**, *24*, 8779. [CrossRef]
22. Barrozo, A.; Orio, M. Unraveling the catalytic mechanisms of H_2 production with thiosemicarbazone nickel complexes. *RSC Adv.* **2021**, *11*, 5232. [CrossRef] [PubMed]
23. Blázquez-Tapias, B.; Halder, S.; Mendiola, M.A.; Roy, N.; Sahu, N.; Sinha, C.; Jana, K.; López-Torres, E. New tin(IV) and organotin(IV) complexes with a hybrid thiosemicarbazone/hydrazone ligand: synthesis, crystal structure and antiproliferative activity. *Bioinorg. Chem. Appl.* **2024**, *2024*, 1018375. [CrossRef]
24. Huedo, C.; Zani, F.; Mendiola, M.A.; Pradhan, S.; Sinha, C.; López-Torres, E. Synthesis, antimicrobial activity and molecular docking of di- and triorganotin(IV) derivatives with thiosemicarbazide derivatives. *Appl. Organomet. Chem.* **2019**, *33*, e4700. [CrossRef]
25. Papadakis, M.; Mehrez, J.; Wehrung, I.; Delmotte, L.; Giorgi, M.; Hardré, R.; Orio, M. Stereochemical tailoring of nickel-based electrocatalysts for hydrogen evolution reaction. *ChemCatChem* **2024**, *16*, e202400426. [CrossRef]
26. Phipps, C.A.; Hofsommer, D.T.; Toda, M.J.; Nkurunziza, F.; Shah, B.; Spurgeon, J.M.; Kozlowski, P.M.; Buchanan, R.M.; Grapperhaus, C.A. Ligand-centered hydrogen evolution with Ni(II) and Pd(II)DMTH. *Inorg. Chem.* **2022**, *61*, 9792. [CrossRef]
27. Barrozo, A.; Orio, M. From ligand- to metal-centered reactivity: Metal substitution effect in thiosemicarbazone-based complexes for H_2 production. *ChemPhysChem* **2022**, *23*, e202200056. [CrossRef]
28. Burón, R.; Jiménez-Gómez, D.; Calatayud, D.G.; Iglesias-Juez, A.; Fresno, F.; Mendiola, M.A.; López-Torres, E. Synthesis, characterization, and photocatalytic activity for water remediation and hydrogen evolution of Zn(II) and Ni(II) bis(thiosemicarbazone) complexes. *Appl. Organomet. Chem.* **2024**, *38*, e7408. [CrossRef]
29. Bilyj, J.K.; Riley, M.J.; Bernhardt, P.V. Isomerism and reactivity of nickel(II) acetylacetonate bis(thiosemicarbazone) complexes. *Dalton Trans.* **2018**, *47*, 2018. [CrossRef]
30. González-García, C.; García-Pascual, C.; Burón, R.; Calatayud, D.G.; Perles, J.; Mendiola, M.A.; López-Torres, E. Structural variety, fluorescence and photocatalytic activity of dissymmetric thiosemicarbazone complexes. *Polyhedron* **2022**, *223*, 115945. [CrossRef]
31. Abrosimov, R.; Moosmann, B. The HOMO-LUMO Gap as Discriminator of Biotic from Abiotic Chemistries. *Life* **2024**, *14*, 1330. [CrossRef] [PubMed]
32. Shittu, F.B.; Iqbal, A.; Ahmad, M.N.; Yusop, M.R.; Ibrahim, M.N.M.; Sabare, S.; Wilson, L.D.; Yantom, D.H.Y. Insight into the photodegradation mechanism of bisphenol-A by oxygen doped mesoporous carbon nitride under visible light irradiation and DFT calculations. *RSC Adv.* **2022**, *12*, 10409. [CrossRef] [PubMed]
33. Jiang, W.-X.; Xie, Z.-L.; Zhan, S.-Z. A photocatalytic system with a bis (thiosemicarbazonato)-nickel over CdS nanorods for hydrogen evolution from water under visible light. *Inorg. Chem. Commun.* **2019**, *102*, 5. [CrossRef]
34. Barca, G.M.J.; Bertoni, C.; Carrington, L.; Datta, D.; De Silva, N.; Deustua, J.E.; Fedorov, D.G.; Gour, J.R.; Gunina, A.O.; Guidez, E.; et al. Recent developments in the general atomic and molecular electronic structure system. *J. Chem. Phys.* **2020**, *152*, 154102. [CrossRef] [PubMed]
35. Hanwell, M.D.; Curtis, D.E.; Lonie, D.C.; Vandermeersch, T.; Zurek, E.; Hutchison, G.R. Avogadro: an advanced semantic chemical editor, visualization, and analysis platform. *J. Cheminform.* **2012**, *4*, 17. [CrossRef] [PubMed]